The role of Nuclear Structure in (some) Reaction Experiments

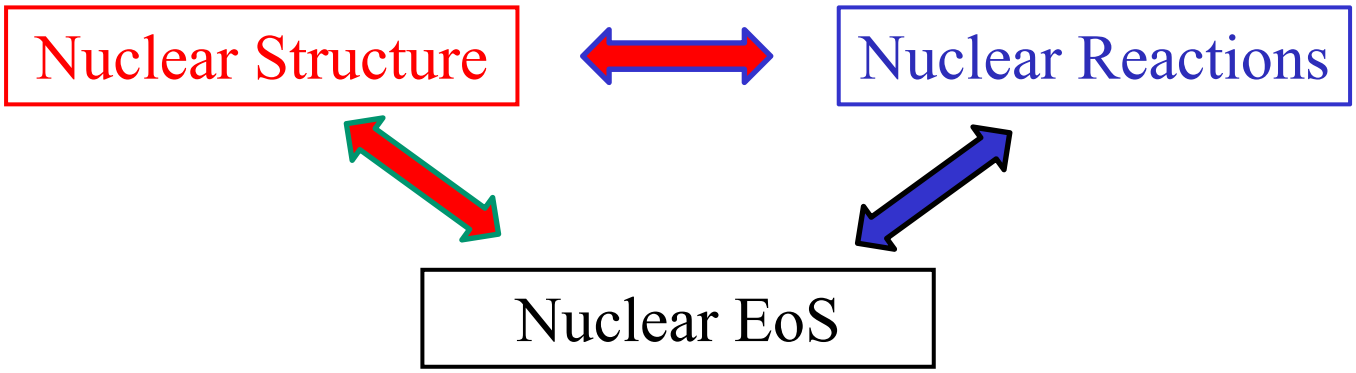

W. Lynch: ECT workshop on Intersection of nuclear structure and high-energy nuclear collisions

Impact of Nuclear Structure on Nuclear Reactions Studies of the EoS

- Studies of collective flow and the high density EoS
- The nuclear liquid-gas phase transition.
- Isospin dependence of the EoS.

Influence of nuclear structure on choices of projectiles and targets for EoS studies

- Most projectiles and targets used in collective flow measurement are spherical. Why? For nuclear structure reasons, they are cheaper.

- We measured flow with a deformed ^{154}Sm target. Why? To convincingly solve a puzzle encountered in collective flow measurements.

Influence of nuclear structure on past choices of projectiles and targets for EoS studies

- The grey and red lines on the chart denote the spherical closed neutron and proton shell nuclei.
- Most projectiles and targets used in flow studies lie near these lines. Why? Basically because of cost.
- To minimize cost of targets and beams, elements with a single stable isotope like gold and niobium were often chosen.
- Experiments with radioactive beams also focused on nuclei with closed proton shells to minimize the changes in ion source technology.

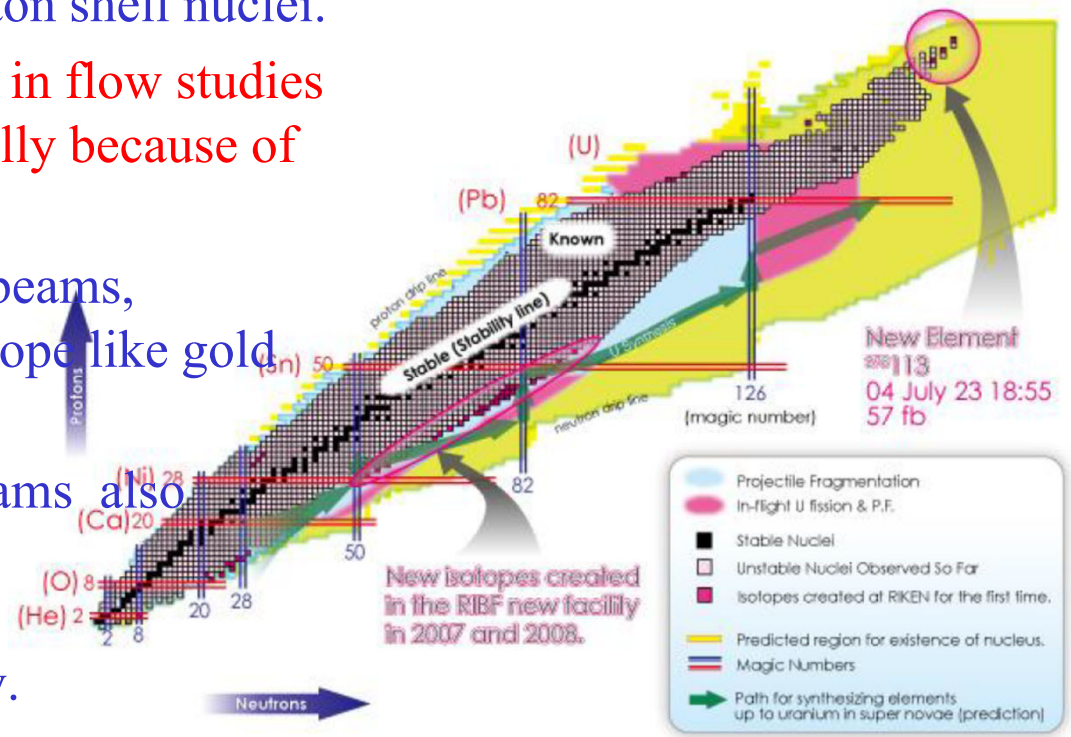

- Deformed nuclei are also a headache in transport theory.
- Nevertheless, we studied flow using a deformed ^{154}Sm target.

Types of flow

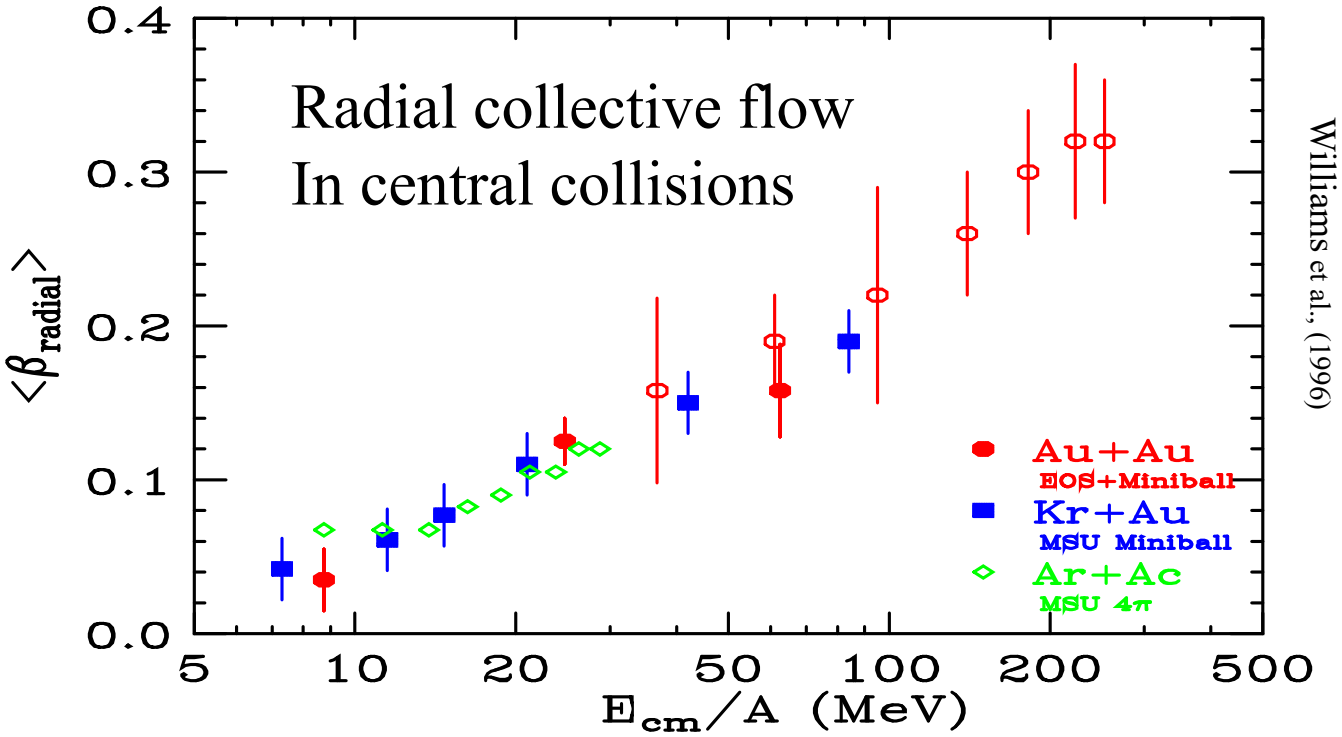

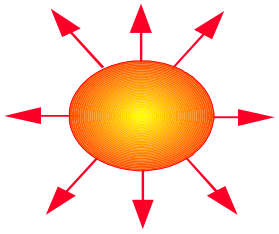

$$\vec{\beta}(\vec{r}) \approx \beta_{\exp} \frac{\vec{r}}{R_{overlap}}$$

$$< KE > \approx < E_{thermal} > +0.3 \bullet A m_N v_{coll}^2$$

•Low energy flow is consistent with Coulomb acceleration of fragmented matter in the C.M. High energy flow reflects compression.

Constraining the EOS at high densities required anisotropic flow

Au+Au collisions E/A = 1 GeV)

Danielewicz, et al., Science 298, 1592 (2002)

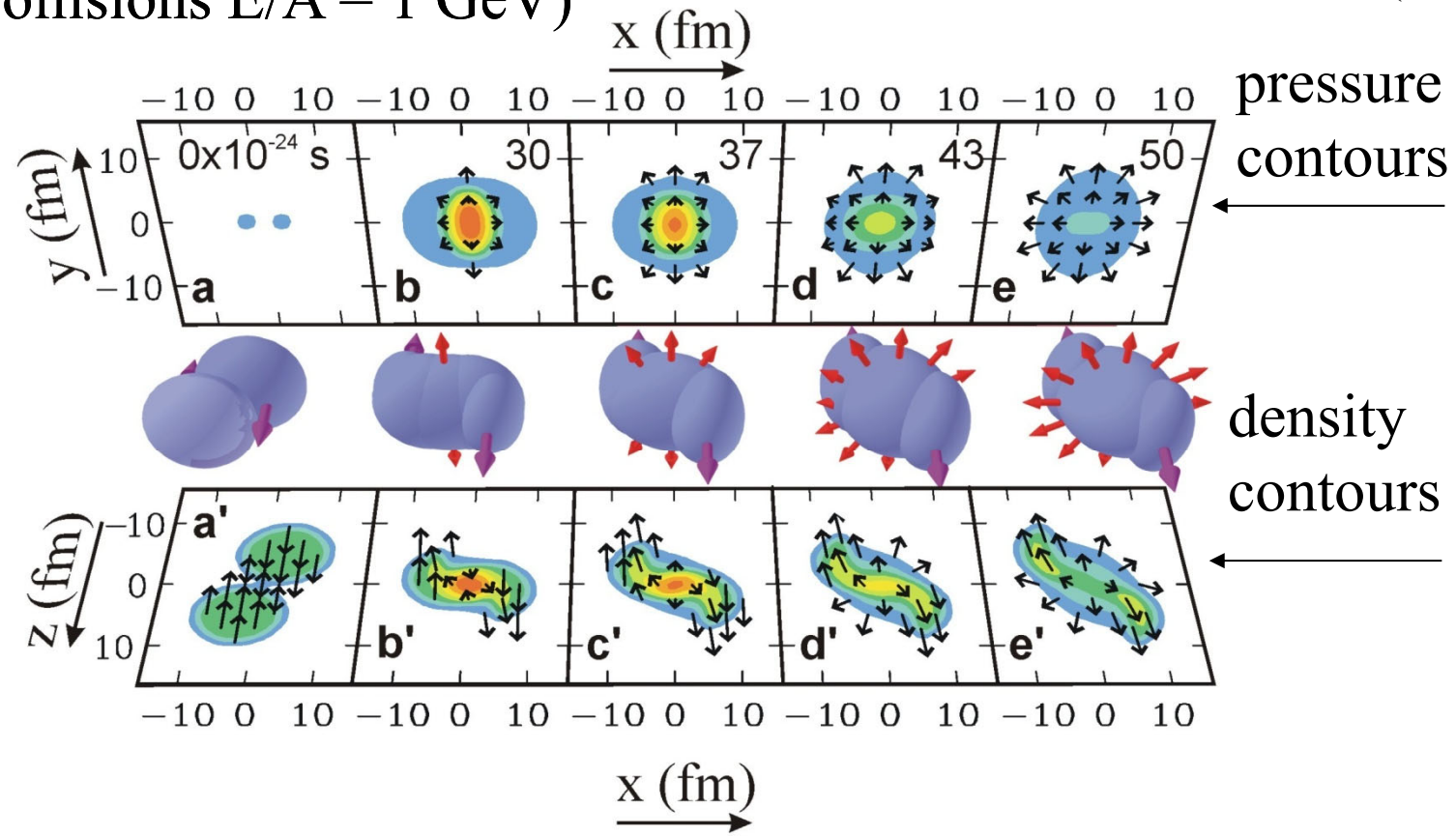

- Two observable consequences of the high pressures that are formed:
  - Nucleons deflected sideways in the reaction plane: V1>0
  - Nucleons are “squeezed out” above and below the reaction plane: V2<0.

Symmetric Matter Constraints

HIC(FOPI),HIC(DLL)

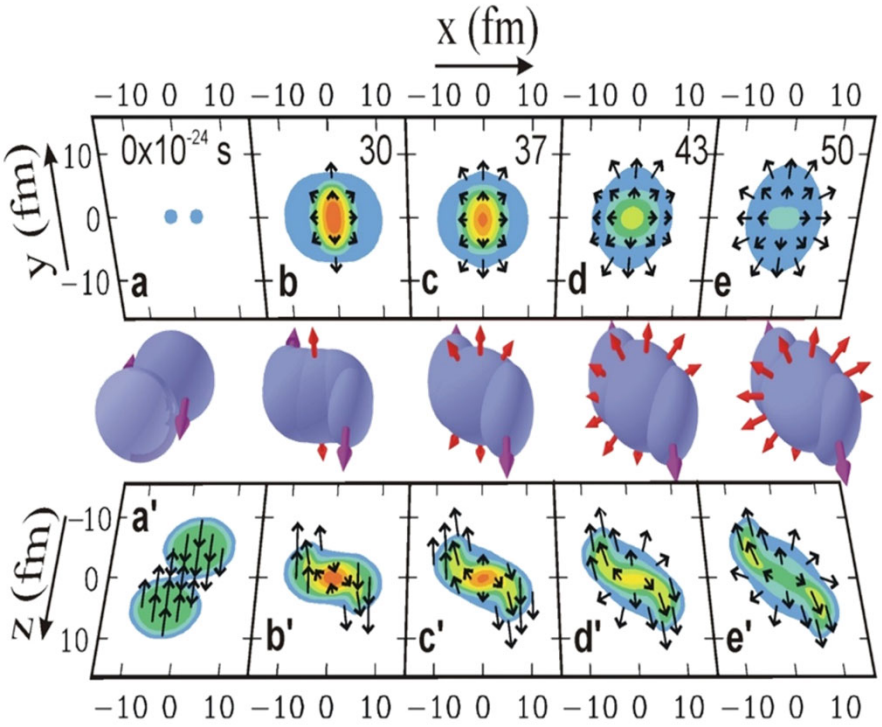

pBUU simulations

Danielewicz, et al., Science 298, 1592 (2002)

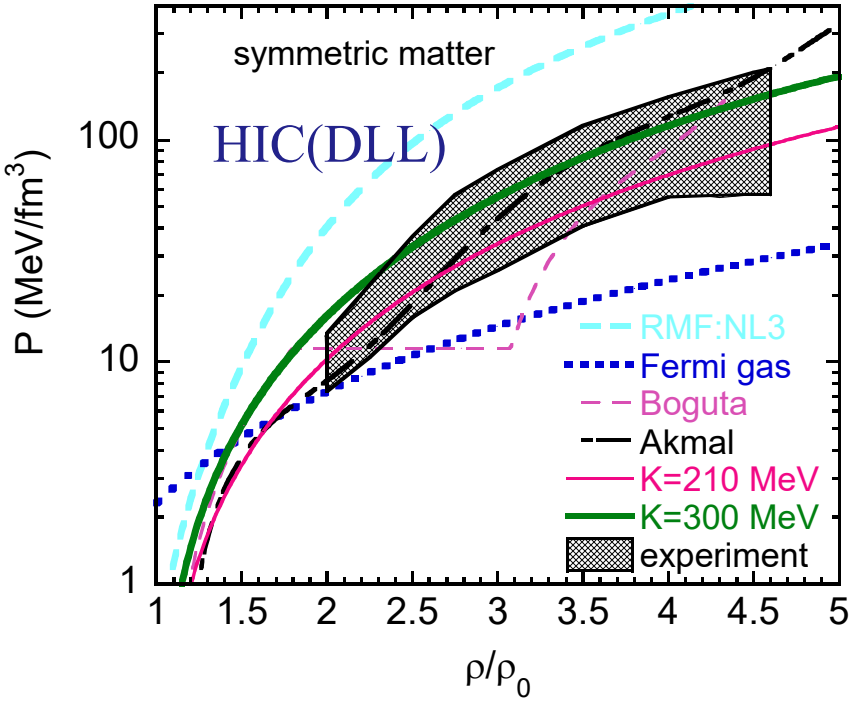

But is this always the correct sign for v1 and v2?

Domination by pressure from collisional heating and mean field repulsion at high densities leads to repulsive flow.

Domination by mean field attraction at low densities leads to attactive orbiting flow

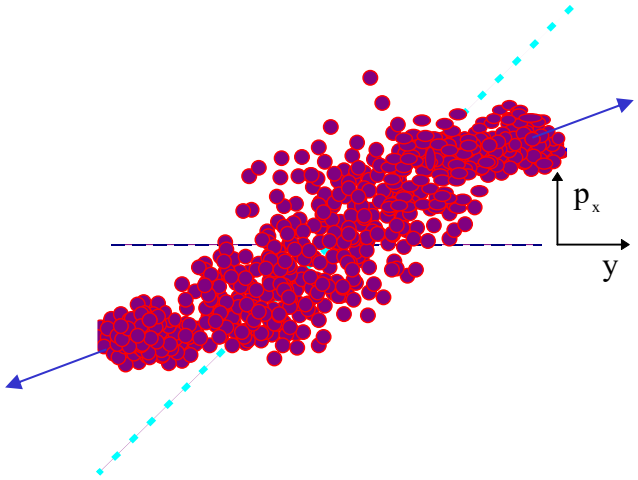

The transverse flow can look similar for repulsive and attractive interactions

Use of nuclear structure to solve a puzzle

- Among the early measurements of collective flow were low energy measurements at MSU for Ar+Sc with the MSU 4π Array. These showed flow attaining a minimum value at E/A 65 MeV.

Westfall et al., PRL 71, 1986 (1993).

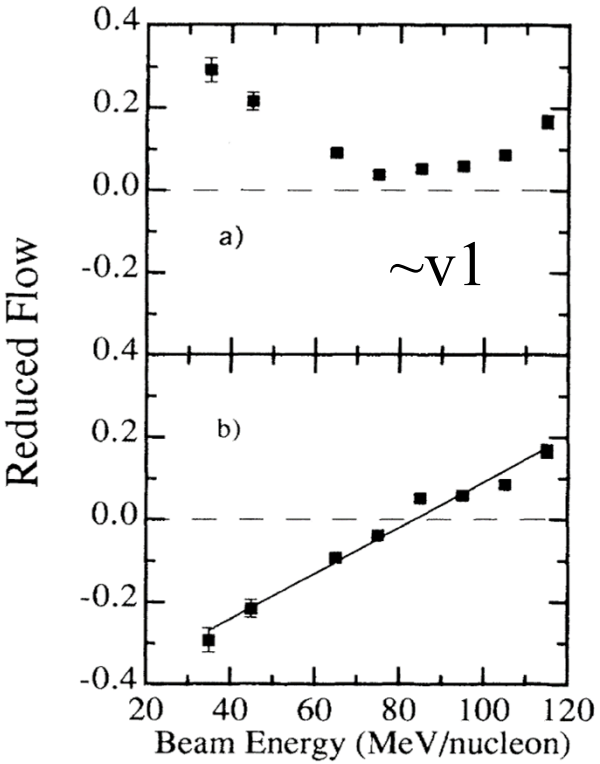

Results for protons from Ar+Sc with MSU 4π array

Reduced flow below 85 AMeV inverted

Solid line is linear fit

- Convention flow analyses cannot distinguish between negative transverse momenta from mean field attraction and repulsive momentum transfers.
- Negative momentum transfer are expected at the lower energies and assumed in the lower figure. How to prove it?

Use of deformed target ^{154}Sm to understand flow

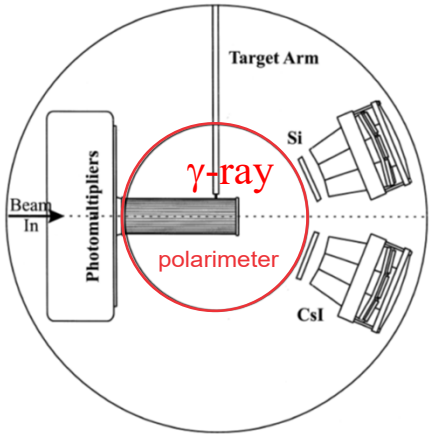

Collisions at non-zero Impact parameter will cause a deformed target to spin.

Circular polarization of γ-rays from heavy deformed residue gives the direction of the orbital angular momentum and sign of the flow.

Westfall et al., PRL 71, 1986 (1993).

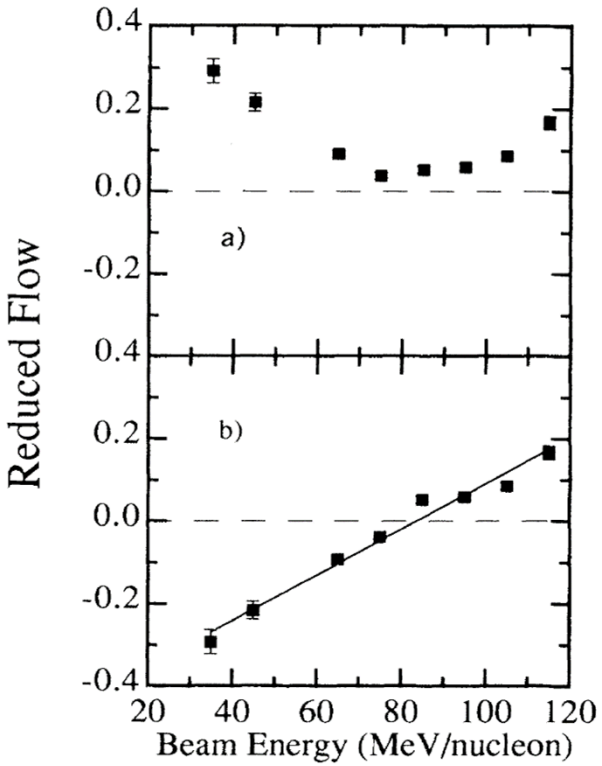

Results for protons from Ar+Sc with MSU 4π array

Reduced flow below 85 AMeV inverted

Solid line is linear fit

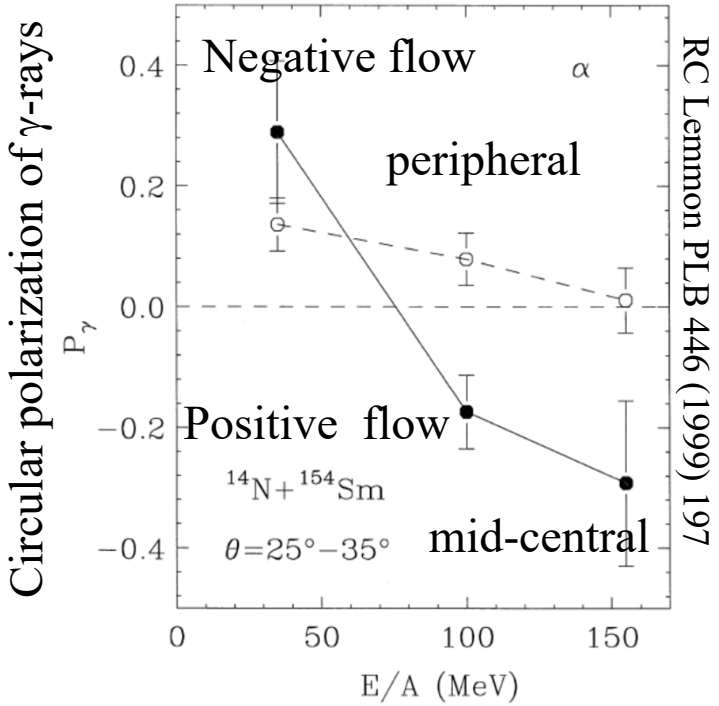

Attractive mean field dominates at low Energies ⇒ flow is negative

Gamma ray polarimeter.

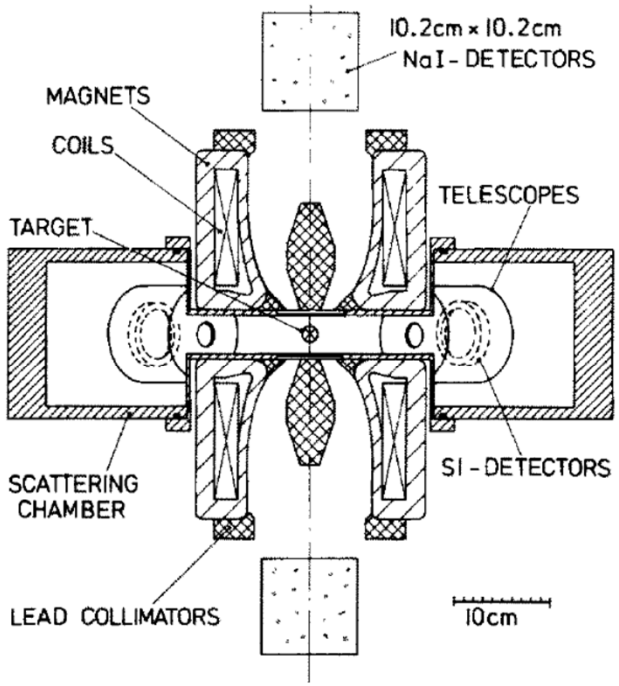

Fig. 1. Doubly symmetric detector setup used in the $^{16}O + ^{48}Ti$ experiments. The figure gives a cross sectional view in the beam direction.

Flow can be well measured and calculated

Transport theory white paper, Sorensen 2023

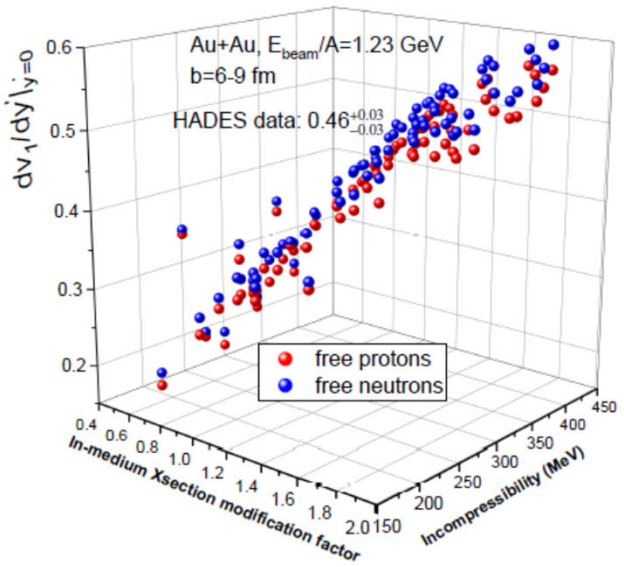

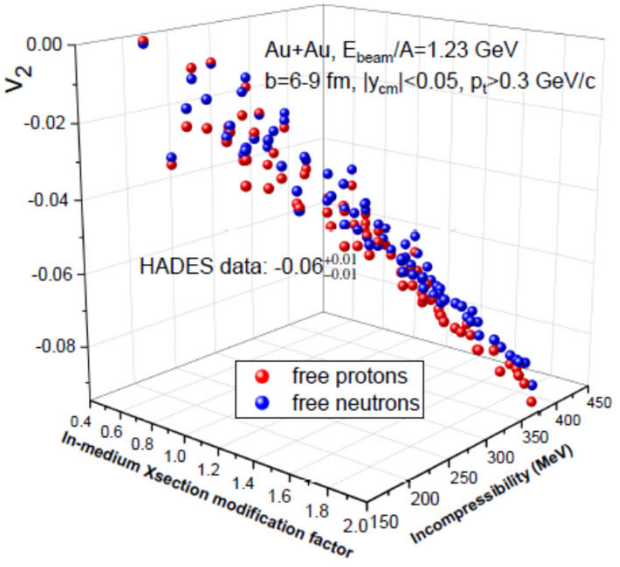

- We saw that flow has provided constraints on the symmetry energy and symmetric matter EoS.
- The figure show the flow for free protons and neutrons measured in Au+Au collisions at E_{beam}/A=1.23 GeV. This is easy to model.
- At lower incident energies, most nucleons are emitted in clusters. The transverse flow for clusters increases significantly with mass as shown below. This mass dependence is not modeled by most transport codes.

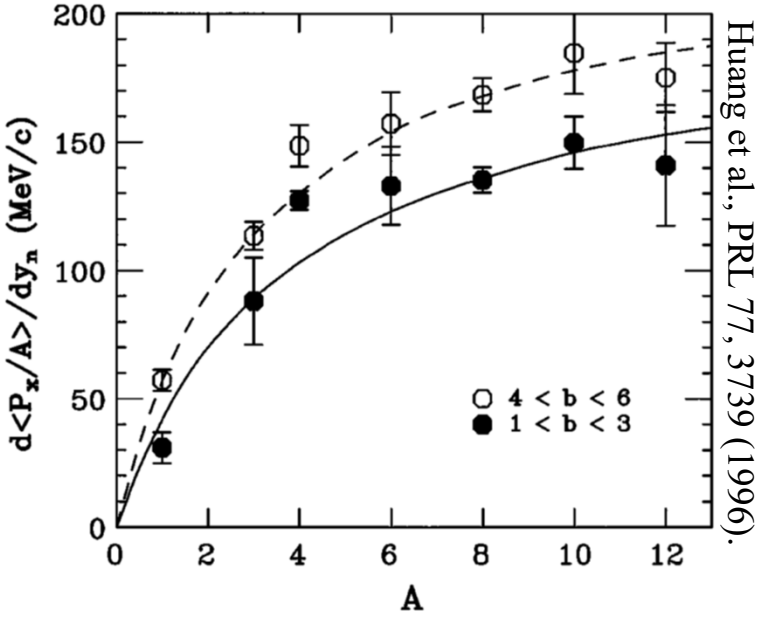

Huang et al., PRL 77, 3739 (1996).

Nuclear structure problem: Cluster production

- Complication: Cluster production influences the calculations of nucleon emission below E/A=400 MeV. Most current transport models don't properly take BE of clusters with A≥4 into account.
- This is not a large problem at high energies where the large entropies suppress the emission of such clusters. If necessary, one can either combine neutrons into clusters at low "freezeout" densities or break them up to make "coalescence invariant" neutron and proton yields, eg. for neutrons:

$$\left.\frac{dM(E_{cm})}{dE_{cm}}\right|_{n,coal.invariant} = \left.\frac{dM(E_{cm})}{dE_{cm}}\right|_{n,free} + \sum_{i_{clust}=1} N_{i_{clust}} \frac{dM\left(E_{cm}/A_{i_{clust}}\right)}{d\left(E_{cm}/A_{i_{clust}}\right)}$$

- To go beyond this approximation, one can increase the number of species in the transport code to include light particles and heavier fragments
- This is challenging because these clusters and fragments do not exist in dense matter. They are produced at $\rho < \rho_0/2$ by nucleation (A<5) and spinodal decomposition (A>3).

M. Oertel, et al Rev. Mod. Phys. 89, 015007-1 (2017)

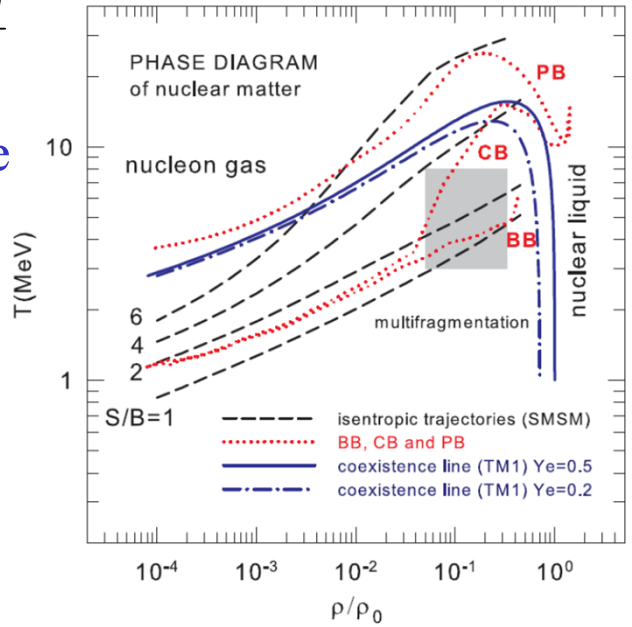

Exception: State of the art AMD transport code that calculates clusters dynamically

Ratios of light cluster spectra

M. Kaneko, A.Ono et al. PLB 822146681 (2021)

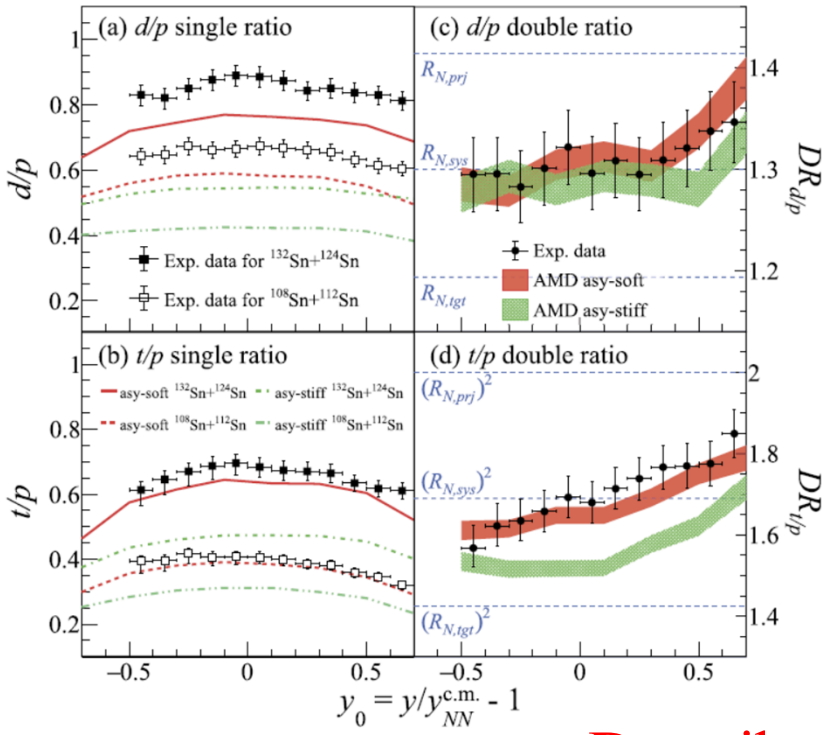

Transport model Symmetry energy functions

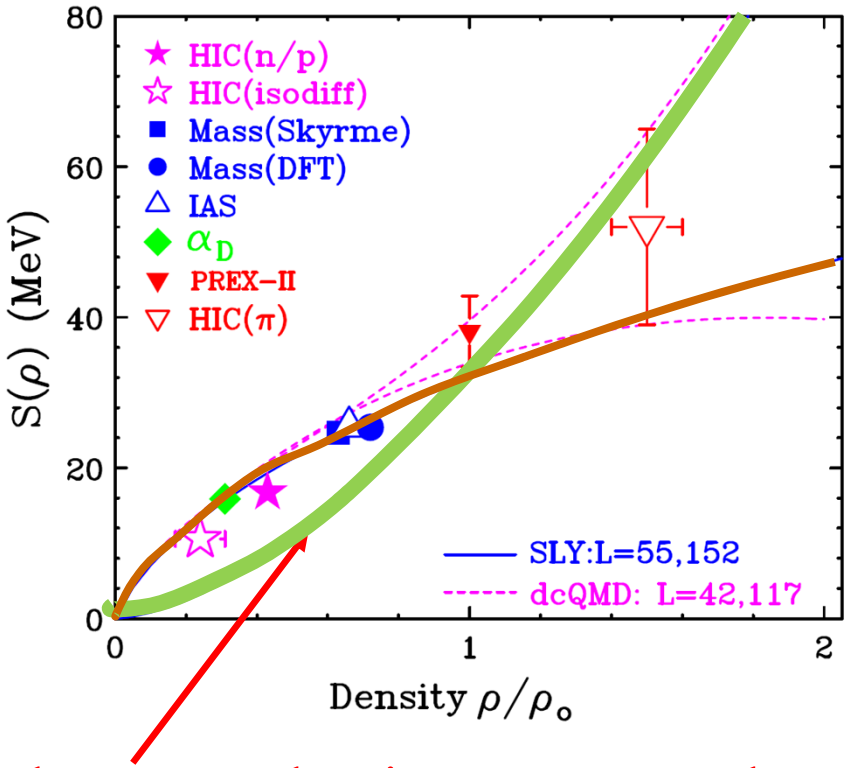

Describes cluster production more poorly

Brown curves are for the SLY L=55 that agrees with EoS

Does the constraints agree with theory? Do they agree with Neutron stars?

Symmetry energy constraints from nuclear physics

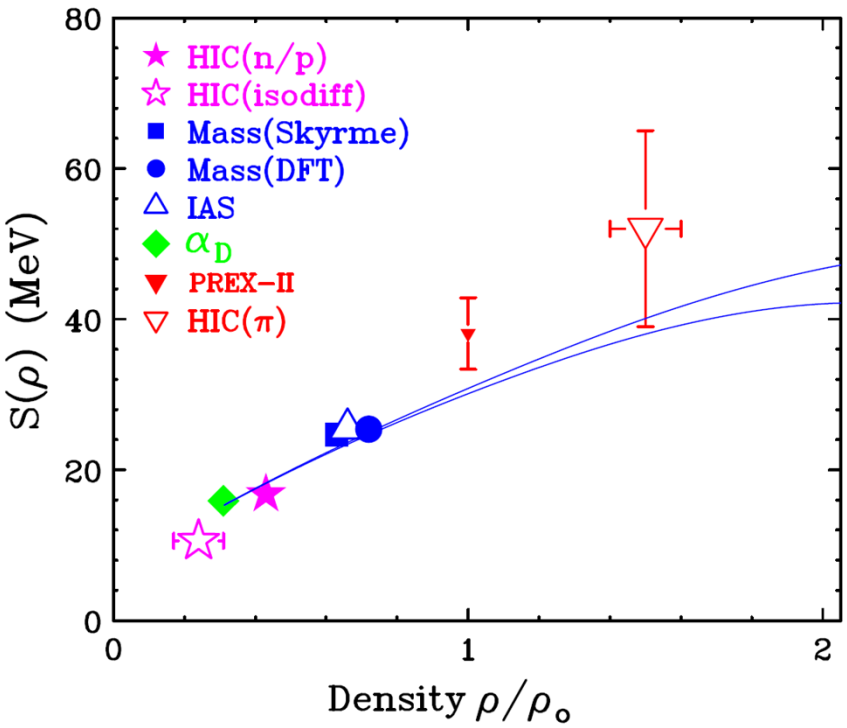

Symmetry energy constraints including neutrons stars

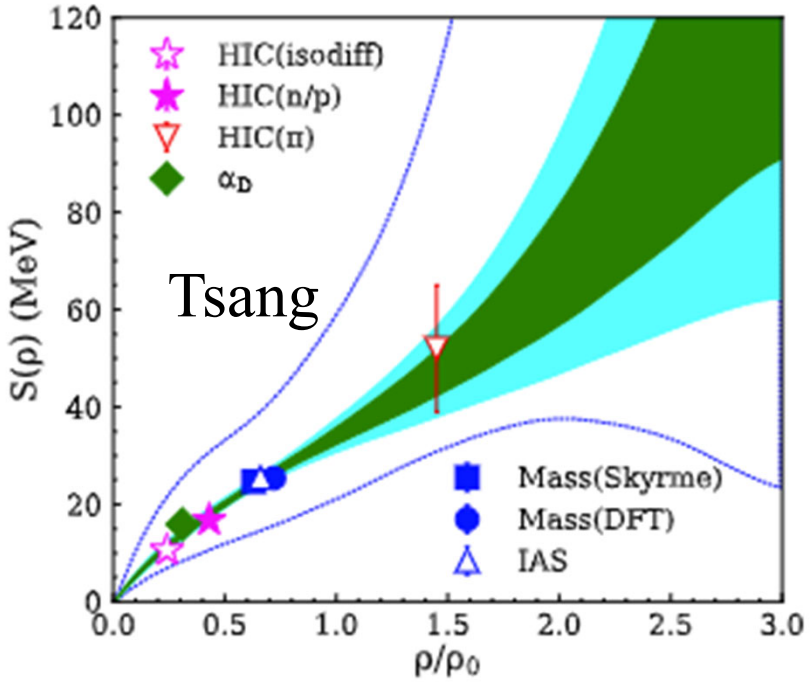

Fragmentation and high temperature EOS

Theoretical tools

Nuclear Statistical Eqilibrium NSE approximation

- Grand canonical, canonical and micro-canonical fragmentation models have been heavily used.
- Some of NSE models developed for fragmentation have also been applied to the supernova EoS.
- Role of structure
- Role of statistical physics

Fragmentation and high temperature EOS

W.A. Friedman Phys. Rev. C 42 (1990) 667.

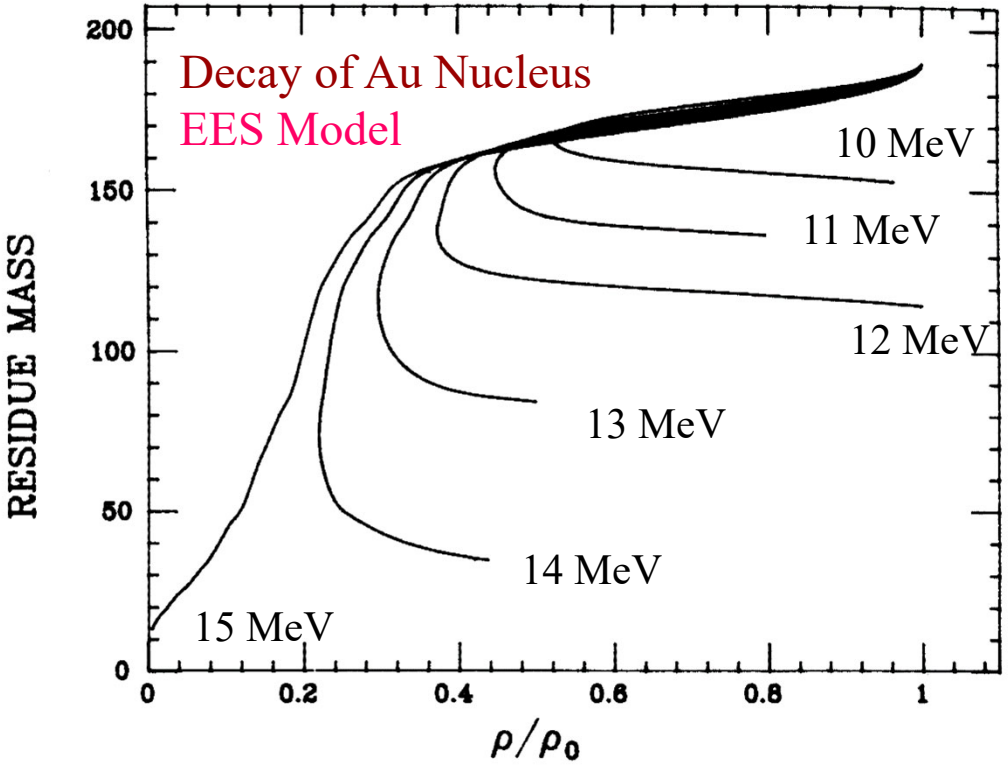

Detailed Balance: $\frac{dN}{dEdt} = const \bullet \sigma_{INV} E \frac{\rho_{daughter}}{\rho_{parent}}$

- Fragment emission rates dramatically increase for $\rho/\rho_0 < 0.4$ where $F(Z_{frag},A_{frag})/A_{frag} < F_{res}/A_{res}$. System decays rapidly to multi-fragment final state with the number of final fragments: $N_{IMF} >> 1$; $3 \leq Z_{IMF} \leq 30$.

Where can multifragmentation be Observed?

- Central HI collisions at 35 MeV≤E/A≤200 MeV.
  - Probe the "participant region formed by overlap of projectile and target.
  - System size constant, in principal.
  - Vaporization observed at high inc. energies.
  - Rapid collective expansion.

- Large-impact parameter HI collisions.
  - Vaporization observed as collision becomes more central.
  - System size impact parameter dependent.
  - Weak collective expansion.
  - Relevant impact parameter limiting fragmetantion increases with incident energy
- Central light ion collisions.
  - Vaporization not observed.
    - Wide E* distribution depending on statistics of high energy cascade.
  - System size constant, in principal.
  - Weak collective expansion.

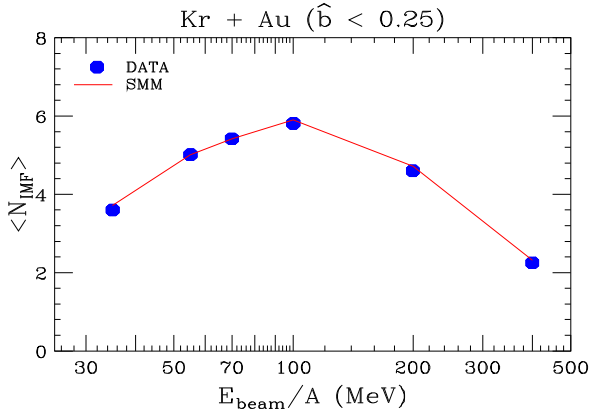

Williams et al., (1997)

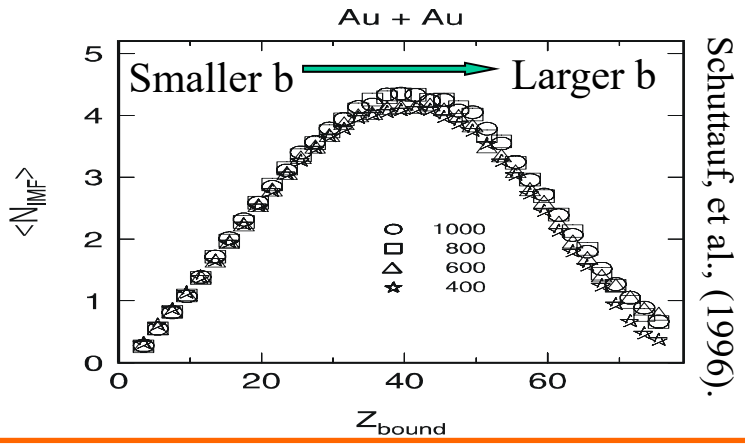

Schuttauf, et al., (1996).

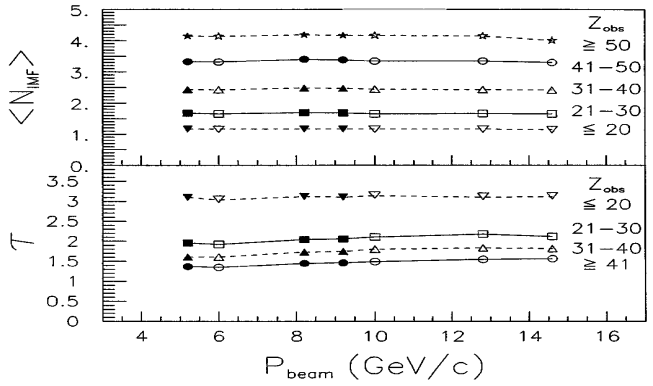

Hsi et al (1997)

Final states velocity distributions for Au+Au Collisions near the multi-fragmentation threshold

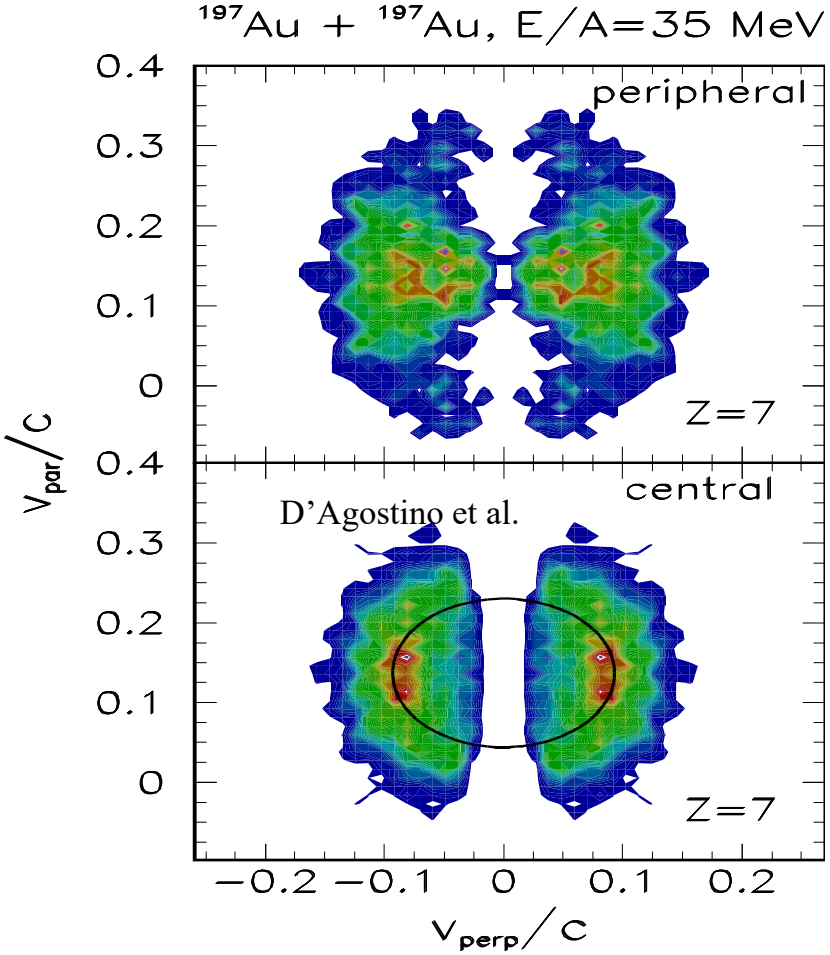

- Peripheral collisions display neck fragmentation and decay of projectile and target residues.

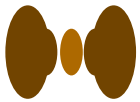

- Central collisions result in multi-fragment breakup with outgoing velocities that are consistent with Coulomb driven expansion from $\rho \approx 0.3\rho_o$.

Application of Nuclear Statistical Equilibrium (NSE) within a two-step Approach

- Assume a rapid first step during which energy is deposited in an equilibrated prefragment.
- Prefragment expands and disassembles according to NSE.
- Excited fragments decouple from system and then decay
- Let's take as ansatz and see what it provides.

Typical Model Parameters:

E^*_{the}/A Thermal excitation energy
Z_{source} Prefragment Charge
A_{source} Prefragment Mass

Because of the first step.

1) $Z_{source} < Z_{tot}$, $A_{source} < A_{tot}$

2) May also need to make some accommodation for collective motion, ⟹ E_{coll}/A, at freezeout.

Comparisons to the NSE Statistical Multifragmentation Model (SMM)

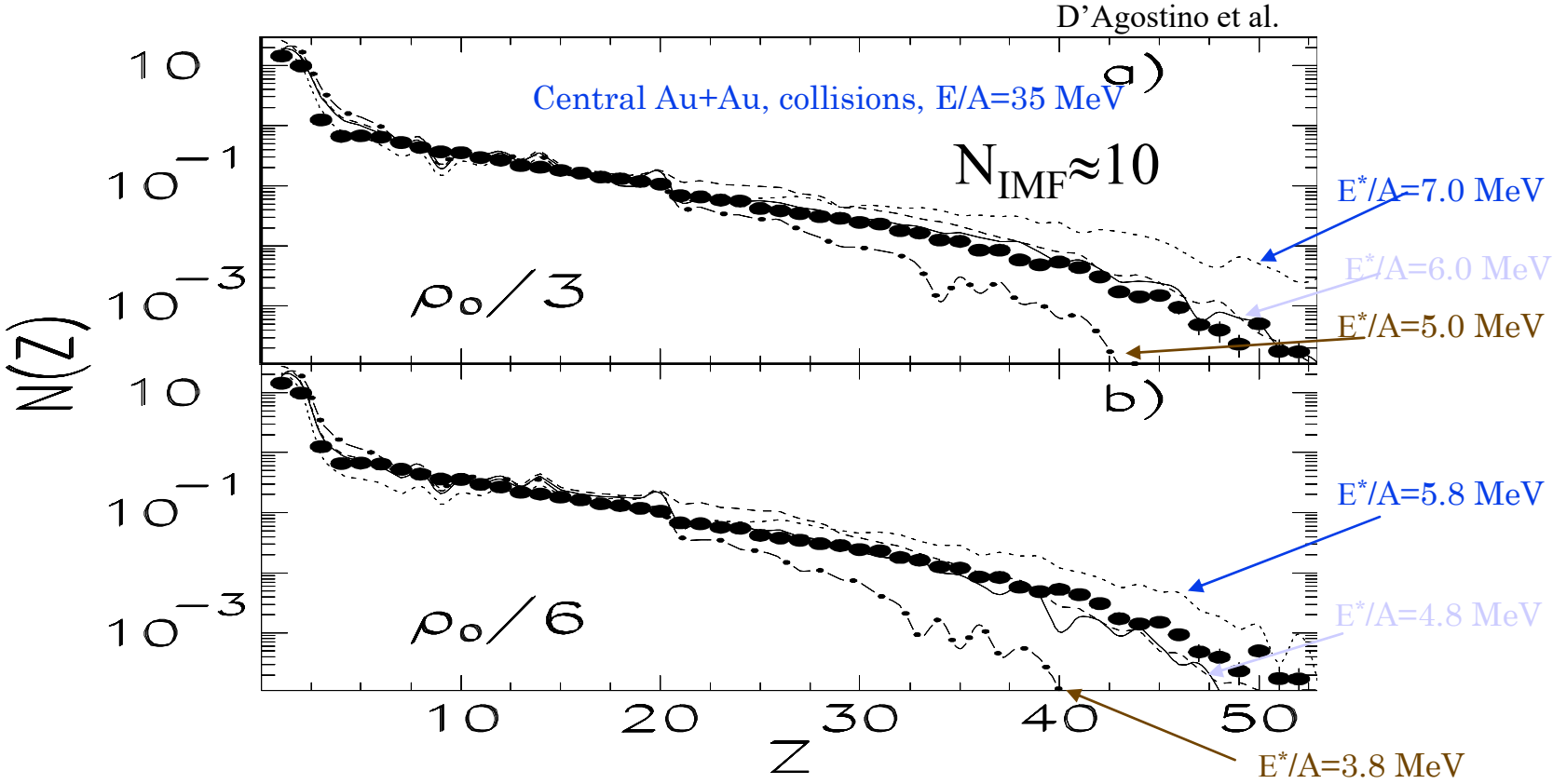

- SMM is a "microcanonical" equilibrium model.
  - Agreement is very good.
  - T ≈ 6 MeV for the calculations, less sensitive to ρ.

Eos from NSE

- If NSE were exactly obeyed and the grand canonical approx. was valid, then number density of nuclei with Z,A would be.

$$n_{A,Z} = \frac{q_{A,Z}}{V} = \frac{g_i \Omega A^{3/2}}{\lambda_T^3} e^{(\mu_B A + \mu_Q Z - f_{A,Z})/T}$$

- Knowing this for all A,Z is equivalent to knowing the EoS.
- If you perform several experiments, with different A and Z, the effective chemical potential can be defined and measured.
- $f_{A,Z}$ is the internal free energy of your nucleus, which is the main unknown.
- You also need to know T and V (or equivalently density) .

Obtaining the free energies

- The free energies are obtained by combining the tabulated experimental level densities to a Fermi gas level densities up the excitation energies sampled in the given experiment.
- The accessible level density is huge and these low lying levels are insignificant fraction of the total.
- They become important because they funnel nearly all decays in to the observed states.

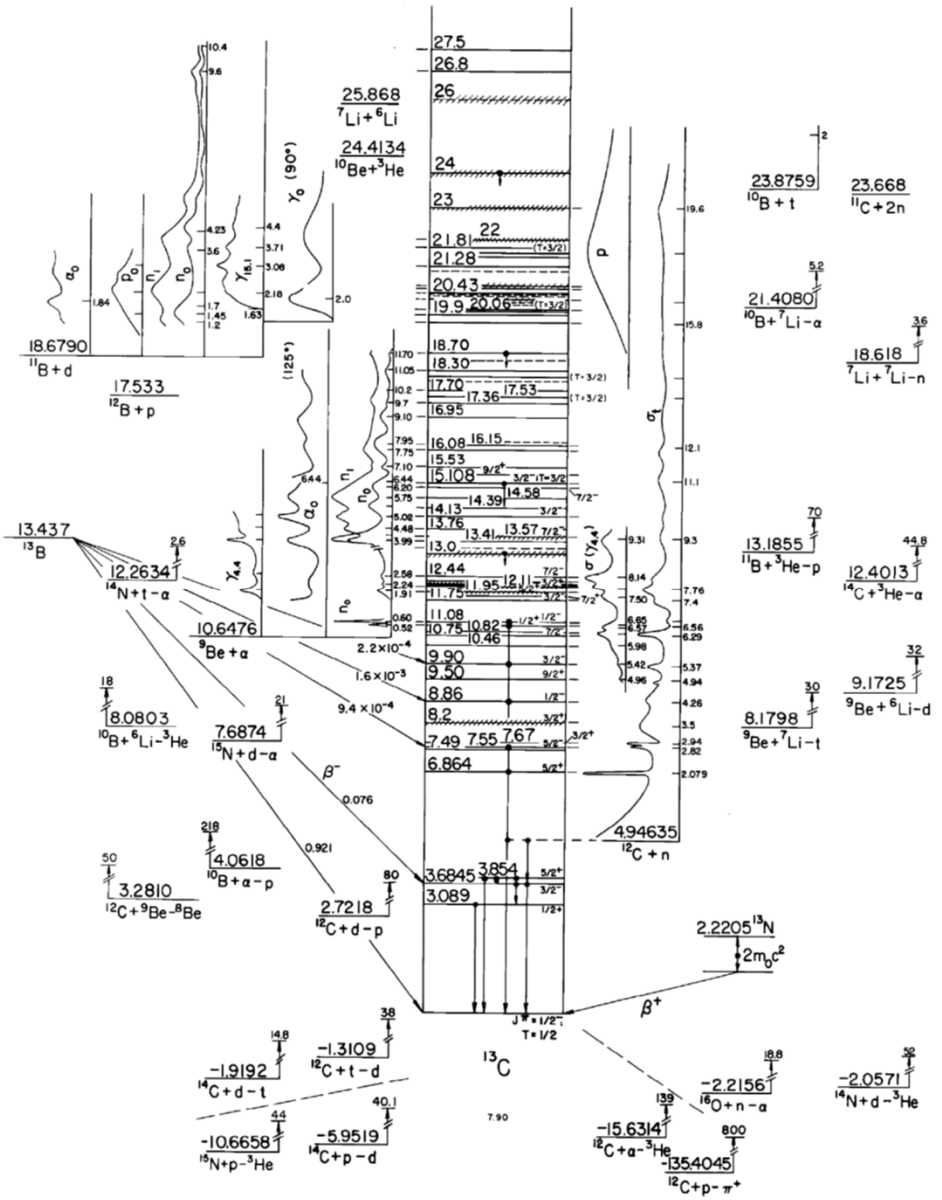

Results for Isotopic Distributions

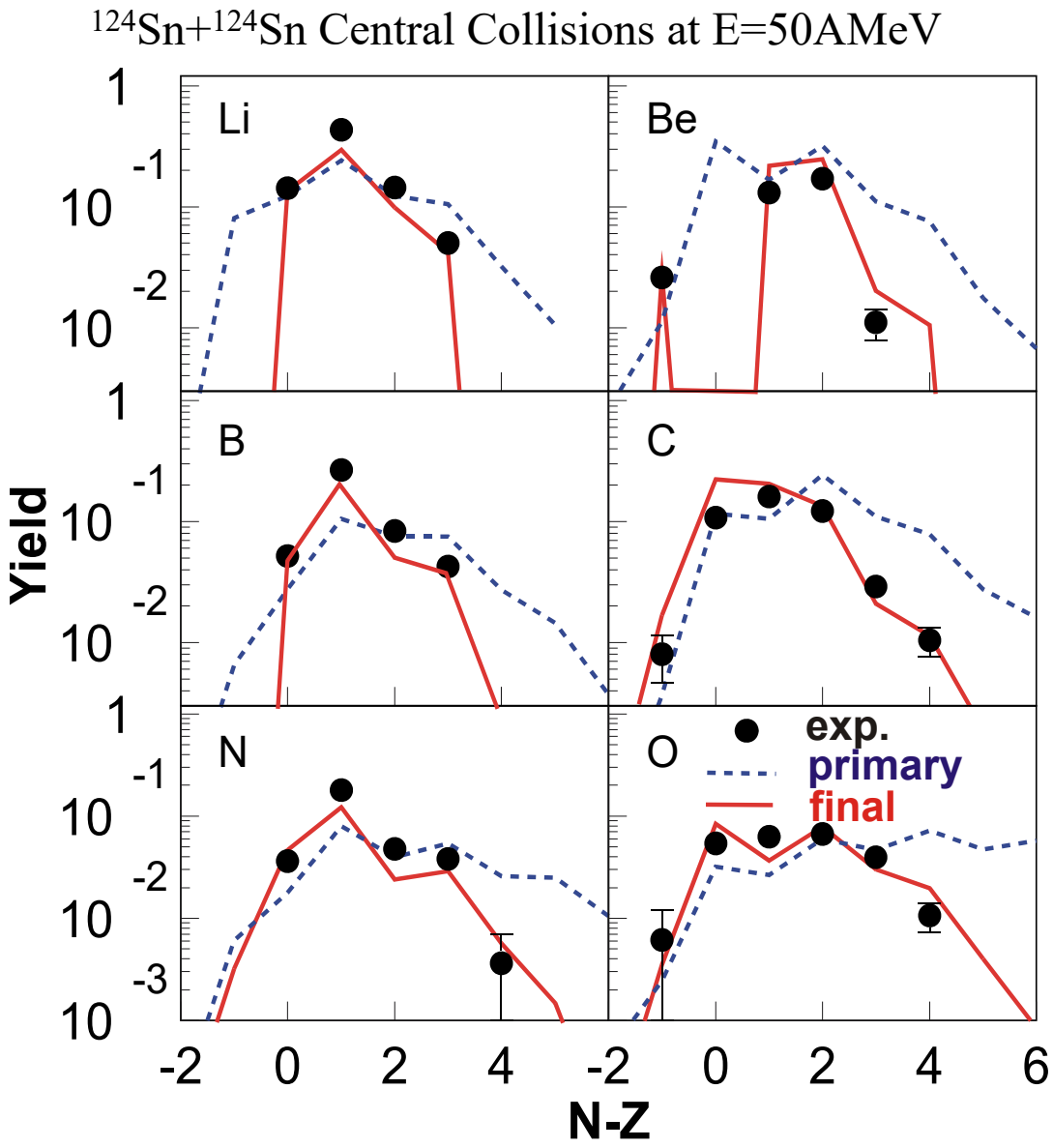

- BUU_SMM calculations
  - BUU: $F_1(u)$, b=1fm
  - SMM: E*/A=4MeV, ρ/ρ_0=1/6
- The shapes and widths of isotopic distributions can be reproduced by the model.

Chemical thermometers”

- Test Chemical Equilibrium: (Benenson...)
  - Excited State Populations:

$$\frac{P_1}{P_2} = \frac{2J_1+1}{2j_2+1}\exp(-\Delta E^*/T)$$

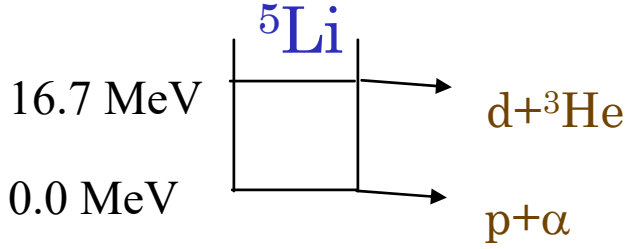

  - Isotope Ratio Temperatures (Albergo...)

$$\frac{Y_1(Z_i,A_i)/Y_2(Z_i,A_i+1)}{Y_3(Z_j,A_j)/Y_4(Z_j,A_j+1)} = a\cdot\exp\left[\left(B_1-B_2-B_3+B_4\right)/T\right]$$

  - This is law of mass action applied to the reaction

$$(Z_i,A_i)+(Z_j,A_j+1)\leftrightarrow(Z_i,A_i+1)+(Z_j,A_j)$$

  - Apparent chemical equilibrium must be corrected for the secondary decay of heavier particle unstable nuclei. Calculations of these corrections are sensitive to the nuclear structure of the emitted fragments.

Use of chemical thermometers to determine freeze-out temperatures

Exited state populations:

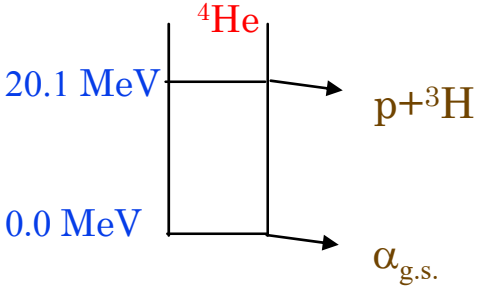

$$\frac{P_1}{P_2} = \frac{2J_1+1}{2j_2+1}\exp(-\Delta E^*/T_{App})$$

Isotope double ratios:

$$\frac{Y_1(Z_i,A_i)/Y_2(Z_i,A_i+1)}{Y_3(Z_j,A_j)/Y_4(Z_j,A_j+1)} = a\cdot\exp\left[(B_1-B_2-B_3+B_4)/T_{App}\right]$$

Au+Au, E/A = 35 MeV
Central collisions
M.J. Huang et al, (1996)

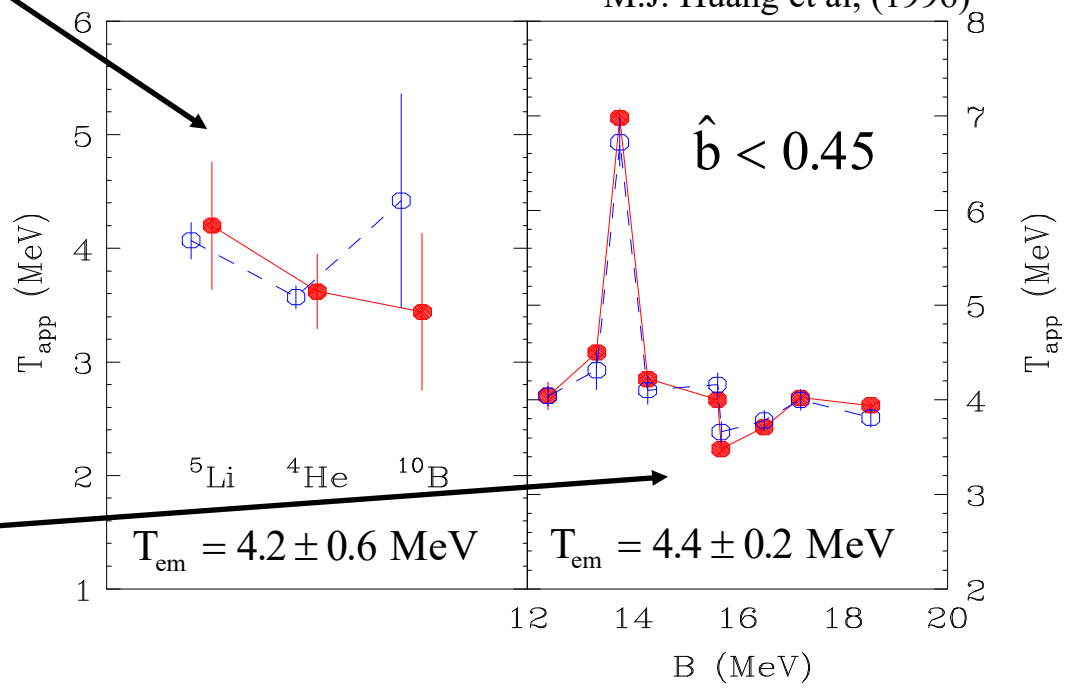

- Excellent consistency with thermal equilibrium for central collisions near the multi-fragmentation threshold
- Deduced temperatures are close to SMM predictions.

Spin determination in multi-fragmentation

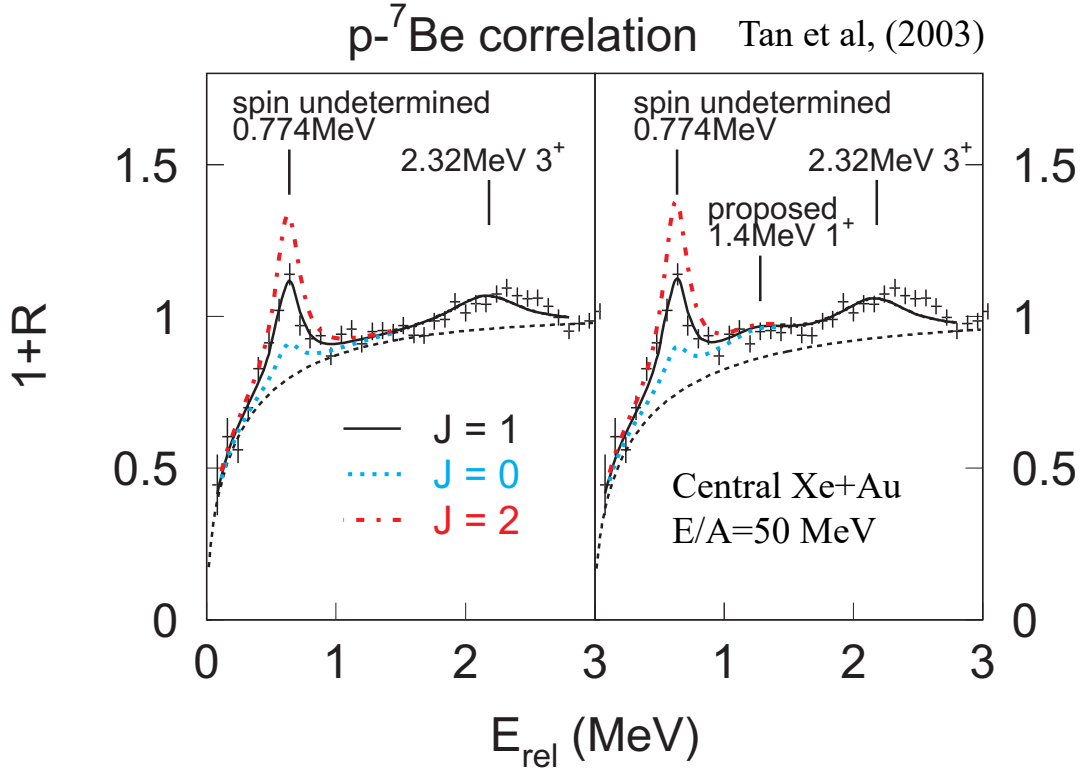

- Even after secondary feeding, the relative populations of nearby states is nearly proportional to (2J+1).
- This allows spin determinations for exotic fragments.
- In other cases one can also measure widths and branching ratios, as well as multi-particle decay modes.

Isoscaling analyses and the symmetry energy

Liu et al.PRC 76, 034603 (2007).

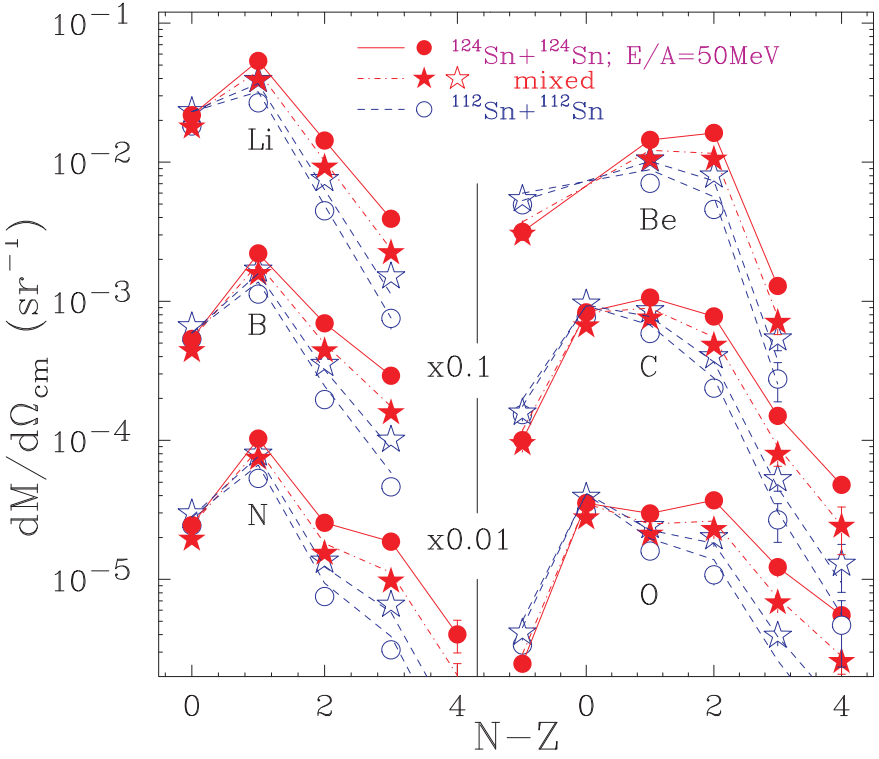

Tsang et. al.,PRL 92, 062701 (2004)

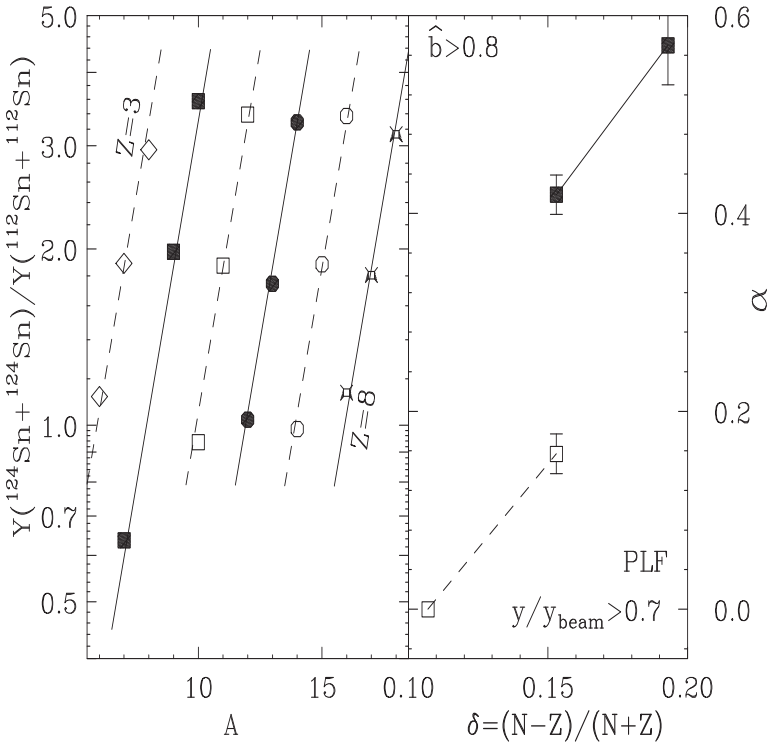

$R_{21}(N,Z)=C_{21}\exp(N\Delta\mu_n/T+Z\Delta\mu_p/T)$ measures the degree to which systems 1 and 2 are out of chemical equilibrium.

In these peripheral collisions, the two reaction partners do not reach chemical equilibrium as indicated by the difference in the shapes of their isotopic distributions and reflected by their chemical potentials.

Summary

- Most nuclear reaction investigations and their conclusions depend strongly on some aspect of nuclear structure.
- Understanding these connections is essential for the science.

Some slides about Bayesian analysis of low density constraints

- There is a wealth of comparisons of low density observables to the symmetry energy. There are also some recent experiments that obtained constraints on the symmetry energy at higher densities. In a recent paper, we determined the sensitive density that was probed by each of these constraints and the symmetry energy or its pressure at that density. Since this came up in the question and answer session. I add a few slides on this point. For future information I encourage interested people to read our recent letter at Lynch and Tsang PLB 830, 137098 (2022).

Methods for EoS Constraints

- Find observables sensitive to Symmetry Energy (SE)
- Determine what each observable constrains such as $S(\rho_s)$, $L(\rho_s)$, $P_{sym}(\rho_s)$ … and at what density or range of densities ρ_s the SE is constrained.
- Choose a technique, such as Pearson correlations, Bayesian inference, crossover technique; you can even obtain the symmetry energy and density from an analysis of the correlations of fit parameters along curves of constant χ^2.
- Find the "sensitive" density ρ_s that is most accurately probed by that observable and the SE at that density

WG Lynch, MB Tsang Physics Letters B 830, 137098 (2022)

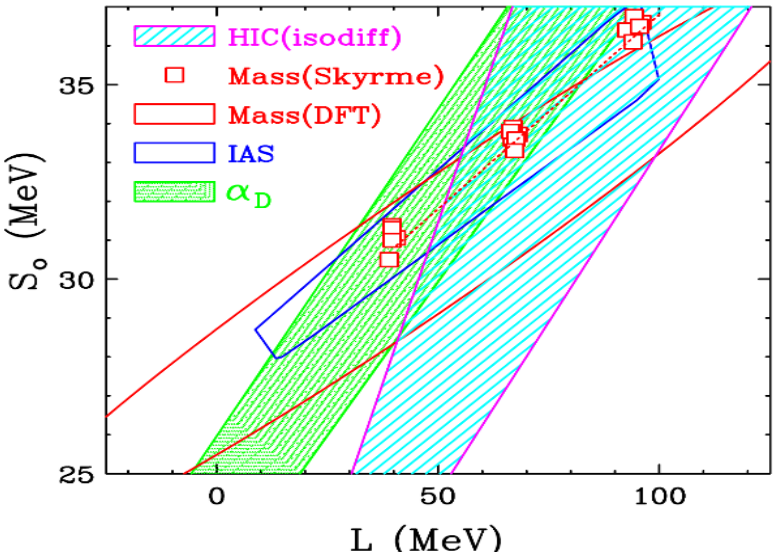

WG Lynch, MB Tsang Physics Letters B 830, 137098 (2022)

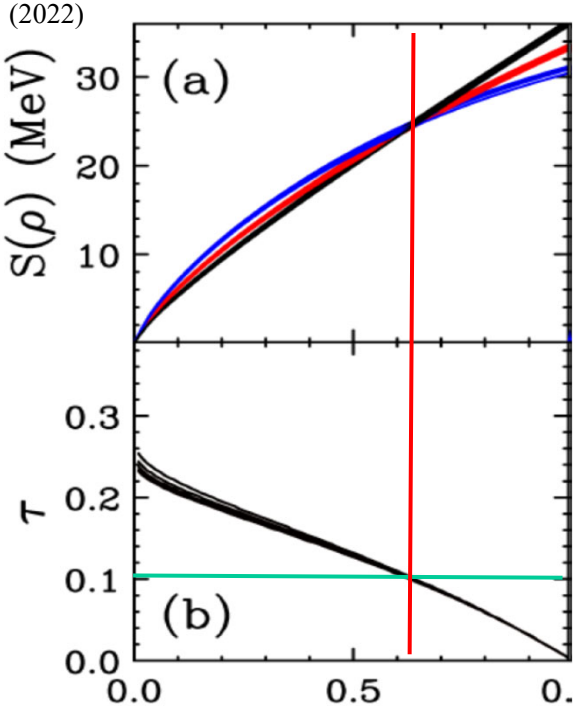

B.A. Brown, Phys. Rev. Lett. 111, 232502 (2013)

Comparison of Crossover and inclination analyses.

$$\tau = \Delta S_0 / \Delta L = -\left(\partial S(\rho_s)/\partial L\right)\Big/\left(\partial S(\rho_s)/\partial S_0\right);$$

τ depends monotonically on ρ_s

If you know the best fit function, the sensitive density can be inferred from the S_0 vs. L contour.

List of constraints on the SE used (not used) to obtain the symmetry energy :

Constraint	ρ/ρ_0	S(ρ) (MeV)	L_{01} (MeV)	L (Mev)	K_{sym} (Mev)	P_{sym} (MeV/fm^3)
Masses	0.63	24.7±0.8				
Masses	0.72	25.4±1.1				
IAS	0.66	25.5±1.1				
HIC (I_{diff})	0.22	10.3±1.0				
α_D	0.31	15.9±1.0				
HIC(n/p)	0.43	16.8±1.2				
PREXII	0.67		71.5±22.6			
HIC(π)	1.45	52±13		79.5±38	47±256	10.9±8.7
HIC(n/p flow)	1.5	24.7±0.8		85±0.8	96±390	12.1±8.4
NICER-P_{SM}	2	24.7±0.8				24±14
NICER-P_{SM}	2	24.7±0.8				72±41
LIGO-P_{SM}	2.5	24.7±0.8				10±7
LIGO-P_{SM}	2.5	24.7±0.8				22±15

W.G. Lynch and M.B. Tsang PLB 830, 137098 (2022)

Constraints that were not used are compared to the results of the Bayesian analyses

Bayesian analysis published in Lynch and Tsang PLB 830, 137098 (2022).

Bayesian determination of SE Compared to Danielewicz IAS+isovector skins

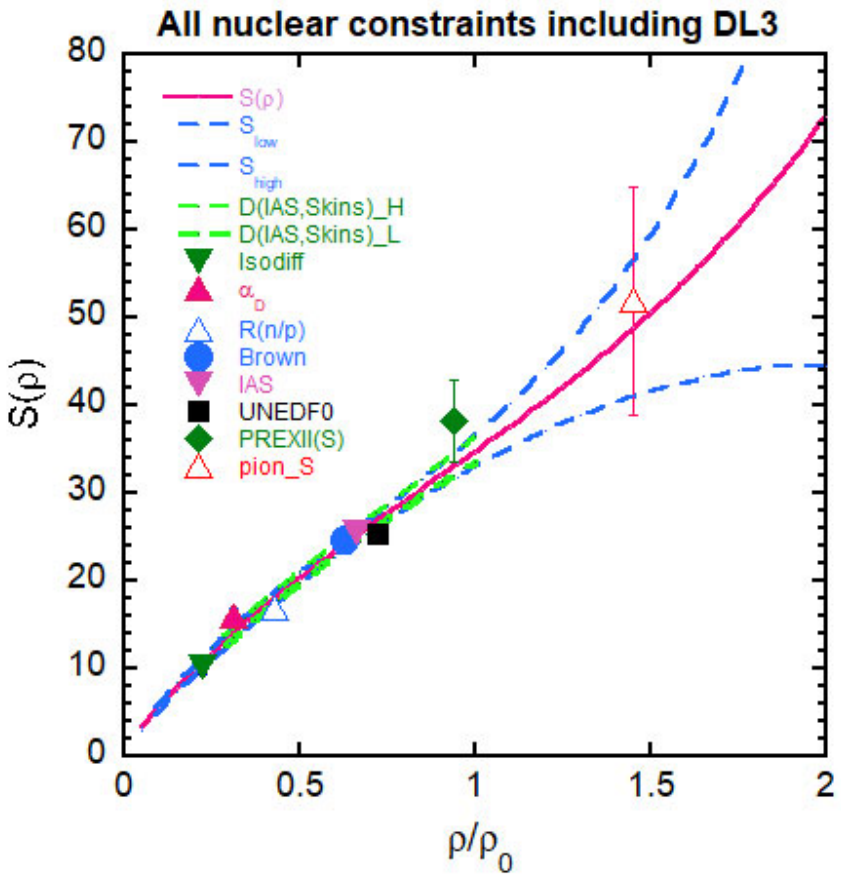

- Danielewicz, Singh and Lee NPA 958, 147 (2017) constrained the symmetry energy at $0.25<\rho/\rho_0<1$ with isobaric analogue states and isovector skins determined from charge exchange reactions.
- The green dashed lines correspond to their 70% confidences limits for the symmetry energy.
- The blue dashed lines correspond to the 70% confidence limits for combined analysis of Lynch and Tsang PLB 830, 137098 (2022).
- The constraint contours for these independent analyses are very similar.